Journal of Power Sources 238 (2013) 336–344

Contents lists available at SciVerse ScienceDirect

Journal of Power Sources

journal homepage: www.elsevier.com/locate/jpowsour

Optimization study of purge cycle in proton exchange membrane fuel cell system

K. Nikiforow*, H. Karimäki, T.M. Keränen, J. Ihonen

VTT – Technical Research Centre of Finland, P.O. Box 1000, FIN-02044, Espoo, Finland

HIGHLIGHTS

- An advanced PEMFC system test bench for anode side studies was built.
- Anode purge gas volume and composition were measured accurately and reproducibly.
- Effect of cathode inlet gas humidification on system performance was studied.
- Mass transport resistance in GDL was found to cause significant voltage polarization.

ARTICLE INFO

Article history:
Received 15 July 2012
Accepted 16 November 2012
Available online 26 March 2013

Keywords:
PEMFC system
Purge cycle
Inert build-up
Hydrogen quality

ABSTRACT

In PEMFC (*proton exchange membrane fuel cell*) systems operating in dead-end mode, hydrogen purges are needed to remove accumulated inert gases and liquid water from the anode side of the fuel cell stack. Hydrogen purges were studied using different humidity levels, purge times, and purge triggering criteria. The purged gas volume and composition were accurately measured with fast data acquisition and an advanced experimental set-up. The experiments were done with constant current density with aim of keeping the anode gas recirculation rate constant. Fuel utilization per pass varied as the hydrogen content on the anode side changed. This study demonstrates how the optimized purge strategy changes with a changing humidity level. It also shows that high fuel efficiency (>99%) is easily reached and that with optimized purge strategy a very high fuel efficiency (99.9%) can be reached. It was also shown that concentration polarization due to accumulation of inert gases on the anode side is two times higher than values obtained by theoretical calculations. This result is significant for purge strategy and system design.

1. Introduction

Proton exchange membrane fuel cells (PEMFCs) are an attractive technology, as they provide zero local emissions, high efficiency and quiet operation. PEMFC technology may provide solutions both for the clean transport as well as stationary applications, such as grid balancing. PEMFC technology has, however, been commercialized only in a limited number of niche applications. Improvements are still required to reduce the cost and to increase the durability of the systems so that mass market applications can be reached.

The design and operation of the anode subsystem, as other PEMFC subsystems, is a sum of many compromises between fuel cell system cost, complexity, efficiency, life-time, and response time. On the other hand, maximization of hydrogen utilization is typically dominated by stack design and system control optimization. Finding energy-efficient system designs to minimize both energy losses due to balance of plant and purged hydrogen is a challenging task.

A common anode subsystem structure in hydrogen fueled PEMFC systems for material handling application and for automotive applications is dead-end operation and valve-controlled hydrogen purge, usually combined with recirculation of the anode gas [1,2]. The hydrogen purge serves two functions. Firstly, it removes some of the inert gases that accumulate in the anode due to permeable membrane and consumption of impure hydrogen [3,4]. Secondly, the purge removes excess water that has accumulated in the anode. Water might accumulate in the anode, even when dry hydrogen is used, due to back-diffusion from the cathode [5].

While the accumulation of inert gas is a relatively simple function of hydrogen quality and membrane permeability, the accumulation of water depends on the stack design and operation conditions [2]. Water accumulation is a major challenge on the

* Corresponding author. Tel.: +358 44 576 2033.
E-mail addresses: kaj.nikiforow@aalto.fi, kaj.nikiforow@vtt.fi (K. Nikiforow).

0378-7753/$ – see front matter © 2013 Elsevier B.V. All rights reserved.
http://dx.doi.org/10.1016/j.jpowsour.2012.11.153

Nomenclature

GDL	gas diffusion layer
LHV	lower heating value (kJ/mol)
PEMFC	proton exchange membrane fuel cell
NLPM	liters per minute of gas at NTP
NTP	normal temperature (0 °C) and pressure (1.013 bar)
E	voltage (V)
E^0	standard voltage, i.e. reversible open circuit voltage at standard state (V)
F	Faraday constant (96,485 C mol^{-1})
ΔH_{H_2}	molar enthalpy change in hydrogen combustion (J mol^{-1})
I	current (A)
n	amount of substance (mol)
p	pressure (bar), 1 bar = 10^5 Pa
Q	volumetric flow rate (NLPM), 1 NLPM = $1.67 \cdot 10^{-5}$ m^3 s^{-1}
R	universal gas constant (8.314 J K^{-1} mol^{-1})
T	temperature (°C), 0 °C = 273.15 K
T_{dew}	dew point temperature (°C)
t	time (s)
V	volume (dm^3 @ NTP)
y	hydrogen mole fraction (−)

Greek symbols

η	efficiency (%)
λ	stoichiometric ratio (−)
Φ_{H_2}	hydrogen utilization per pass (%)
ψ_{H_2O}	fraction of water leaving the system as liquid water through the anode (%)

Subscripts

a	after a purge
an	anode
b	before a purge
cat	cathode
cool	coolant
f	in the fresh hydrogen feed
in	anode/cathode/coolant inlet
out	anode/cathode/coolant outlet
p	purge/in the purged gas

cathode side, and there are numerous studies of the topic, most of which are included in Anderson's review [6].

System efficiency optimization as a function of purged hydrogen and fuel quality has been modeled by Ahluwalia and Wang [1]. In their study, the fuel quality and the membrane thickness determining the nitrogen flux from the cathode were varied. In this optimization study, the accumulation of liquid water was neglected, even if it is known to be a significant cause of inhomogeneity in fuel cell stacks [7].

Recently, Promislow et al. modeled the optimum bleed rate for anode gas [8]. While the work of Promislow et al. points out many important aspects, such as the time scale to reach the steady state nitrogen level and the importance of the dilution effect of anode nitrogen, it is based on several assumptions that are difficult to achieve in practical systems. As the authors point out, uniform current density is assumed and the effects of water management are neglected.

The accumulation of nitrogen and water and their effects have been studied both at the single cell [9–12] and the stack or system level [13–19]. Both of these approaches serve a certain purpose. While the studies that use a single cell give more accurate results for flow field geometry, the studies that use a stack bring out the problems due to uneven flow distribution between the cells.

While many of these studies provide valuable information for the stack design and for system design and operation, data is lacking of the amount of hydrogen purged when the system is operated with realistic control parameters. The amount of purged hydrogen is measured by Adegnon et al. [15], but the purge time is several seconds, while in practical systems it is a fraction of a second. It is also important to quantify how much of the water is actually removed from the anode channels by the purge in different operating conditions. Only the study by Dehn has measured this [2].

In this work, development of a novel experimental set-up enabling measurement of both the purged gas volume and the hydrogen content of the purged gas in a dead-end operated system is reported. Purged volume and fuel utilization were experimentally studied using different purge strategies and different humidity levels of cathode air. Water balance for the system operating in constant current conditions was measured, including the liquid water leaving the system through the anode during a purge. Concentration polarization due to liquid water and nitrogen accumulation was measured and compared to theoretical polarization due to simple gas dilution.

2. Experimental

2.1. Fuel cell system test bench

The PEMFC system test bench reported in a previous study [13] was modified to enable accurate recording of anode side system behavior during purges and also to enable control of the cathode humidity level.

A high data sampling rate during the purge was enabled using a trigger signal from the PEMFC control system just before the control system triggers the purge. The sampling rate during anode purge was increased from 2 Hz to 50 Hz not more than 1 s prior to opening the purge valve and was maintained until 10 s had elapsed since closing the purge valve. A hydrogen mass flow meter (Alicat MS-500SLPM) with fast response time (10 ms) was added to the fuel inlet line. The use of this mass flow meter enabled accurate measurement of the hydrogen flow rate during the purge. The hydrogen concentration sensor, placed in the slipstream in the previous study [13], was replaced with two more stable hydrogen concentration sensors (Applied Sensor HPS-100), which were placed at the inlet and outlet of the anode main line.

The humidification level of the cathode gas was controlled by adding a by-pass line, enabling only a fraction of the inlet air to flow through the humidifier. The by-passed air flow rate was measured with mass flow meter (TSI 42350101).

In addition to these changes in the instrumentation, the aged commercial Nedstack P8 stack used in the previous work was replaced with a latest generation Nedstack P8 stack. A scheme of the experimental set-up is shown in Fig. 1.

2.2. Test procedure and test matrix for purge measurements

The measurements were made using a constant current and constant cathode flow rate and pressure, as the cathode was not pressurized. The current level corresponded to a high efficiency point ($E_{cell,avg}$ = 660–690 mV) and the air stoichiometric ratio (λ_{air} = 2.5)

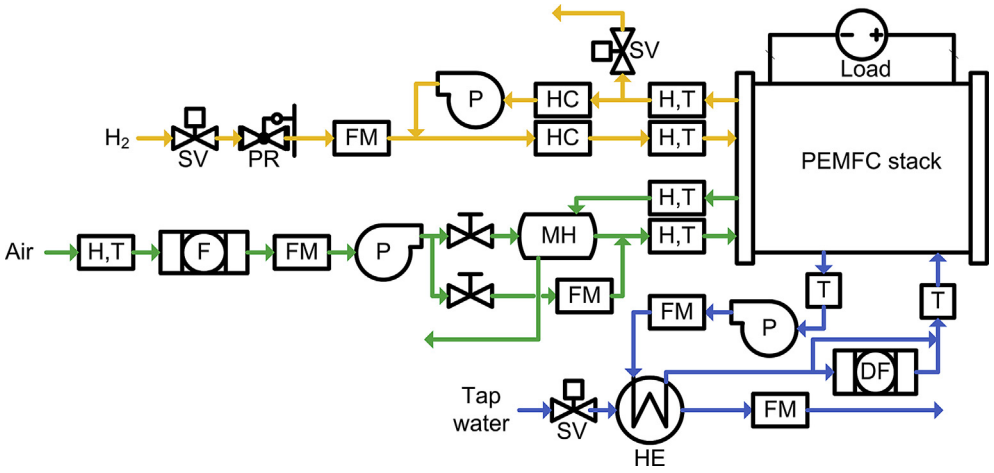

Fig. 1. Scheme of the system test bench. DF: de-ionization filter, F: filter, FM: flow meter, H: humidity measurement, HC: hydrogen concentration measurement, HE: heat exchanger, MH: membrane humidifier, P: pump/blower, PR: pressure regulator, SV: solenoid valve, T: temperature measurement.

was close to optimum from the system efficiency point of view. The hydrogen recirculation rate was maintained at its maximum to enable an even humidification on the anode side even under dry conditions. The anode inlet overpressure ($p_{an,in}$ = 200 mbar) was chosen based on previous experience and was a compromise between durability, fuel efficiency, and the ability of the purge gas to remove liquid water. The operating conditions are shown in Table 1.

Prior to conducting the measurements, the system was allowed to stabilize, i.e. it was operated until the hydrogen mole fractions in the anode line had reached a pseudo-steady state. Once the system had stabilized 10 consecutive purge cycles were recorded, during which the liquid water leaving system through purge valve was collected and measured. The length of one purge cycle varied between 3 and 22 min, depending mainly on the voltage drop allowed between purges. Using the humidity measurements and the measured amount of liquid water leaving the system through the anode purge valve, the total amount of water leaving the system could be determined by establishing a water balance. In Fig. 2 one complete measurement is presented and variations of the parameters are shown.

The measurement routine was repeated by varying (1) the cell-average voltage drop that triggers an anode purge ($\Delta E_{trigger}$ = 3, 6, 9 mV), (2) the cathode inlet dew point temperature ($T_{dew,cat,in}$ = 52, 55, 58 °C), and (3) the time the purge valve was kept open (t_p = 200, 400 ms).

The matrix of measurements performed in this work is shown in Table 2. Measurements performed in high humidity conditions and

Table 1
Measured time average operating conditions and parameters.

Parameter	Target	Measured time average
I_{stack}	120 A	119.9–120.0 A
$Q_{an,in}$ [a]	–	107–113 NLPM
$p_{an,in}$	200 mbarg	186–217 mbarg
$p_{an,out}$	–	146–180 mbarg
Fuel quality	–	99.9% H_2 [b], <20 ppm H_2O
$Q_{cat,in}$	319 NLPM	321–329 NLPM
λ_{O_2}	2.5	2.52–2.58
$p_{cat,in}$	–	75–84 mbarg
$p_{cat,out}$	–	10–15 mbarg
$T_{cool,in}$	60–60.5 °C	60.1–60.5 °C
ΔT_{cool}	–	2.8–4.1 °C

[a] Total anode gas flow rate including recirculation.
[b] The fuel quality was determined using the method described in Karimäki et al. [13].

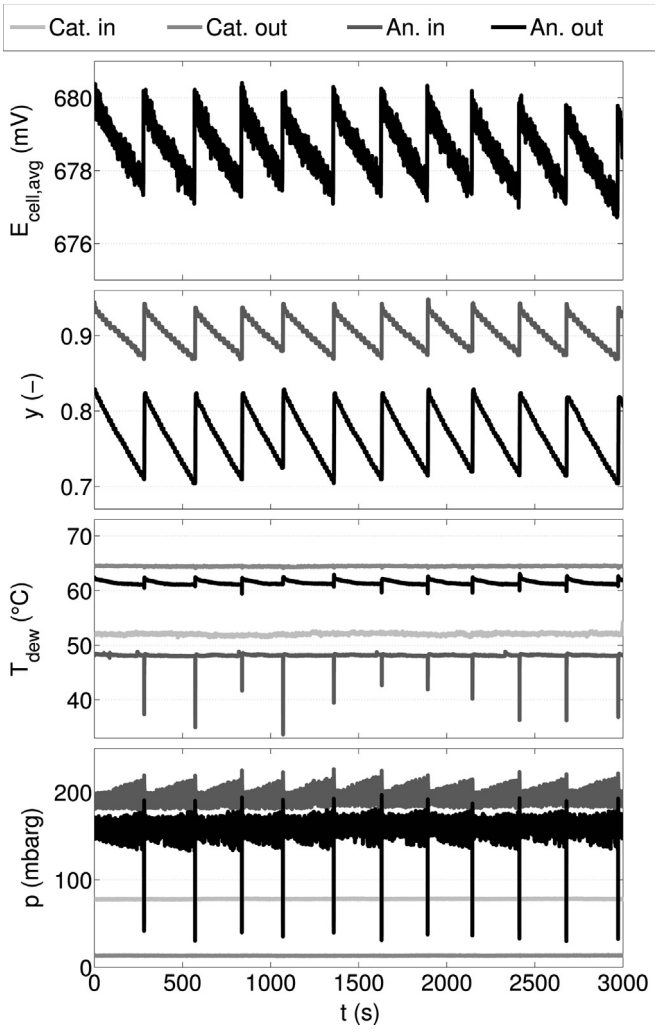

Fig. 2. Average cell voltage ($E_{cell,avg}$), hydrogen mole fractions (y), dew point temperatures (T_{dew}), and pressures (p) during one complete measurement. The cathode inlet dew point temperature is $T_{dew,cat,in}$ = 52 °C, the purge time is t_p = 400 ms, and the purge triggering criteria is $\Delta E_{trigger}$ = 3 mV.

Table 2
Test matrix and the number of successfully measured consecutive purge cycles. Three data sets are numbered and their ordinals are shown as superscripts.

↓ $\Delta E_{trigger}$ (mV)	The number of successfully measured consecutive purge cycles					
$T_{dew,cat,in}$ (°C)/t_p (ms) →	52/200	55/200	58/200	52/400	55/400	58/400
3	$6^{1,2,3}$	7^{1}	7^{1}	$9^{1,2}$	$9^{1,3}$	9^{1}
6	$7^{2,3}$	0	0	8^{2}	9^{3}	0
9	$7^{2,3}$	0	0	7^{2}	9^{3}	0

long purge intervals were shown to be challenging because of unstable performance of the stack due to extensive water accumulation. Reliable data from these measurements was not acquired. Instead, the results from the three data sets numbered in Table 2 are addressed.

2.3. Analysis of purged gas volume and composition

Analysis of the purged gas volume and the hydrogen mole fraction in the purged gas was performed using the measured flow rate profile of hydrogen entering the anode and the hydrogen concentration in the anode line before and after the anode purge.

Fig. 3 shows a typical hydrogen flow rate (Q) profile and anode inlet hydrogen mole fraction (y) change during an anode purge. As seen from the figure, there is a time lag between closing the purge valve and the measured maximum flow rate. The observed time lag is due to the opening and closing times of the valve, which result in anode gas being purged after giving the command to close the purge valve. Furthermore, the hydrogen flow rate profile is wider than the time the valve is kept open. This is explained with the principles of fluid dynamics in that a flow caused by a pressure gradient evens out the pressure gradient, thus resulting in a decreased fluid flow rate.

The volume of fresh hydrogen entering the anode during a purge is calculated by numerically integrating the hydrogen flow rate profile over time, as follows:

$$V = \int Q_{feed} dt \tag{1}$$

This volume equals the volume of anode gas purged (V_p) and can be converted into moles of gas purged (n_p) using the ideal gas law, as follows:

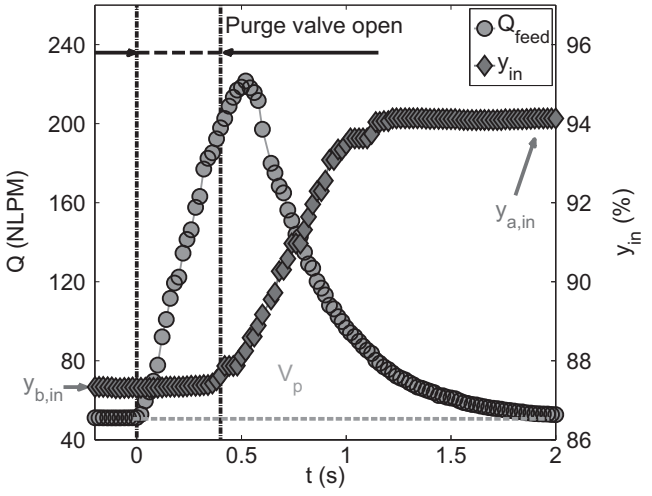

Fig. 3. Hydrogen flow rate (Q) and anode inlet hydrogen mole fraction (y_{in}) during anode purge. The cathode inlet dew point temperature is $T_{dew,cat,in}$ = 52 °C, the purge time is t_p = 400 ms, and the purge triggering criteria is $\Delta E_{trigger}$ = 3 mV.

$$n_p = \frac{p \cdot V_p}{R \cdot T} \tag{2}$$

The purged gas is a mixture of hydrogen, nitrogen, and water and the mole fraction of hydrogen (y_p) can be determined by establishing a mole balance for the purge process by using Eqs. (1) and (2), the measured hydrogen mole fractions in the anode line ($y_{b,in}$, $y_{a,in}$, $y_{b,out}$, $y_{a,out}$), and the mole fraction of hydrogen in the feed (y_f), as follows:

$$y_p = y_f - \frac{n_{an}}{n_p} \cdot (y_a - y_b) \tag{3}$$

In Eq. (3), y_b and y_a are the average hydrogen mole fractions in the anode line before and after the purge, respectively. They are calculated using $y_{b,in}$, $y_{b,out}$, $y_{a,in}$, $y_{a,out}$, and fractional volumes of anode gas at inlet and outlet concentrations. The fractional volumes of anode gas at different concentrations were determined by measuring the anode volume as described by Nikiforow [20]. n_{an} in Eq. (3), represents the moles of gas in the anode line and is calculated based on the anode line volume, temperature, and pressure using the ideal gas law (Eq. (2)). Eq. (3) is valid when it can be assumed that the temperature and pressure of the purged gas equal the temperature and pressure of the fresh hydrogen and that all compounds in the anode gas behave like an ideal gas.

When losing as little hydrogen as possible during an anode purge, y_p should equal $y_{b,out}$. In practice, however, this is seldom true because part of the excess fresh hydrogen entering the anode during a purge and mixing with the recirculated anode gas often makes it to the purge valve while it is still open. In this case, the purged gas can be thought of as a mixture of (1) fresh hydrogen and (2) anode outlet gas, and the fraction of fresh hydrogen (n_f) purged to the purged gas (n_p) can be expressed as follows:

$$\frac{n_f}{n_p} = \frac{y_p - y_{b,out}}{y_f - y_{b,out}} \tag{4}$$

Using Eq. (4), the amount of additional hydrogen compared to $y_{b,out}$ lost during a purged can be determined.

3. Experimental results and discussion

3.1. Effect of humidity level on purged volume and gas composition

During the experiments, the humidity level used was found to have a significant effect on the purged gas volume and composition. As discussed in Section 2.2, the measurements with the highest humidity level were troublesome to perform. Therefore, only measurements with lowest trigger voltage (3 mV) are used in this analysis.

In Table 3, the measured time average reactant dew point temperatures in both stack inlet and outlet, as well as the hydrogen mole fractions in both stack inlet and outlet, are shown. In Table 4, the calculated volume of anode gas purged, anode gas recirculation rate at the anode inlet, average hydrogen utilization per pass, and fraction of water leaving the system as liquid water through the

Table 3
The measured time average reactant dew point temperatures (T_{dew}) and average hydrogen mole fractions in anode loop before and after a purge (y). The purge triggering criteria was $\Delta E_{trigger} = 3$ mV.

↓ $T_{dew,cat,in}$ (°C)	$T_{dew,cat,in}$ (°C)		$T_{dew,cat,out}$ (°C)		$T_{dew,an,in}$ (°C)		$T_{dew,an,out}$ (°C)		y_b (−)		y_a (−)	
t_p (ms) →	200	400	200	400	200	400	200	400	200	400	200	400
52	52.1	52.0	64.7	64.4	47.6	48.1	60.4	61.4	0.78	0.80	0.85	0.88
55	54.9	54.9	64.9	64.9	49.5	49.7	62.5	62.9	0.73	0.77	0.79	0.85
58	58.0	58.0	65.4	65.5	50.3	51.1	64.0	64.1	0.59	0.73	0.65	0.80

Table 4
The calculated volume of anode gas purged (V_p), anode gas recirculation rate at anode inlet ($Q_{an,in}$), average hydrogen utilization per pass ($\Phi_{H_2,average}$), and fraction of water leaving the stack as liquid water on the anode side (ψ_{H_2O}). The purge triggering voltage drop was $\Delta E_{trigger} = 3$ mV.

↓ $T_{dew,cat,in}$ (°C)	V_p (dm^3 @ NTP)		$Q_{an,in}$ (NLPM)		$\Phi_{H_2,average}$ (%)		ψ_{H_2O} (%)	
t_p (ms) →	200	400	200	400	200	400	200	400
52	1.03	1.88	112.5	109.7	55.8	55.9	0.1	0.3
55	0.50	1.32	111.5	110.8	59.4	56.9	3.1	3.6
58	0.26	0.74	108.2	112.4	70.3	58.4	6.5	7.3

anode are shown. All data presented in Tables 3 and 4 are averaged from the number of successfully measured consecutive purge cycles shown in Table 2. The anode gas recirculation rate at anode inlet presented in Table 4 is determined as described by Nikiforow [20].

The hydrogen flow rate profiles averaged from all successfully measured consecutive purge cycles are shown in Fig. 4. As seen from these figures, the higher the humidity level, the lower the peak flow rate and the longer it takes for the flow rate to respond to the opened purge valve. These observations suggest that flow resistance increases significantly with increasing the humidity level, i.e. with increasing liquid water accumulation in the flow channels. The increased flow resistance, in turn, results in less gas being purged. This is seen in Fig. 5, where the volume of gas purged as a function of humidity level is shown.

The mole fraction of hydrogen in the purged gas (y_p) as a function of humidity level and n_f/n_p as a function of humidity level and purged volume are shown in Figs. 6 and 7, respectively. Fig. 6 suggests that y_p approaches the hydrogen mole fraction at the anode outlet before the purge ($y_{b,out}$) when increasing the humidity level. This is quite intuitive because when the humidity level increases, the purged volume decreases (Fig. 5) and, thus, less fresh hydrogen entering the anode during purge reaches the purge valve. With the increasing humidity level and, thus, with the increasing flow resistance, a condition is eventually encountered where the fresh hydrogen entering the anode during the purge does not reach the purge valve. In this condition, the purged gas has the same composition as the anode outlet gas before the purge ($y_p = y_{b,out}$), the fuel efficiency reaches its maximum, and the fraction of fresh hydrogen in the purged gas is zero. This condition is approached, as shown in Fig. 7a. Assuming plug flow and no back flow from the recirculated gas, the volume of anode gas purged equals the volume between anode outlet and the purge valve (Fig. 7b).

When increasing the humidity level and decreasing the purge time, measurements become increasingly inaccurate because of the unsteady and unreliable behavior of the stack under these conditions. This means that while maintaining the purged volume below the limit when $y_p = y_{b,out}$ is desirable from the fuel efficiency point of view (because the maximum dilution of the purged gas is achieved), it may result in inefficient liquid water removal. Thus, minimizing the amount of hydrogen lost in a purge might not be the optimal solution for system performance, especially if the system is operated in high humidity conditions.

The measurements in the current set-up show that the fuel efficiency (η_{fuel}) does not play a very central role in the total efficiency ($\eta_{total} = \eta_{fuel} \cdot \eta_{stack}$) but instead the stack efficiency (η_{stack}), dominated by the stack humidity level, is the controlling factor. The efficiencies are calculated as follows:

$$\eta_{fuel} = \frac{n_{H_2,consumed}}{n_{H_2,consumed} + n_{H_2,purged}} \quad (5)$$

$$\eta_{stack} = \frac{2 \cdot F \cdot E_{stack}}{-\Delta H_{H_2,LHV}} \quad (6)$$

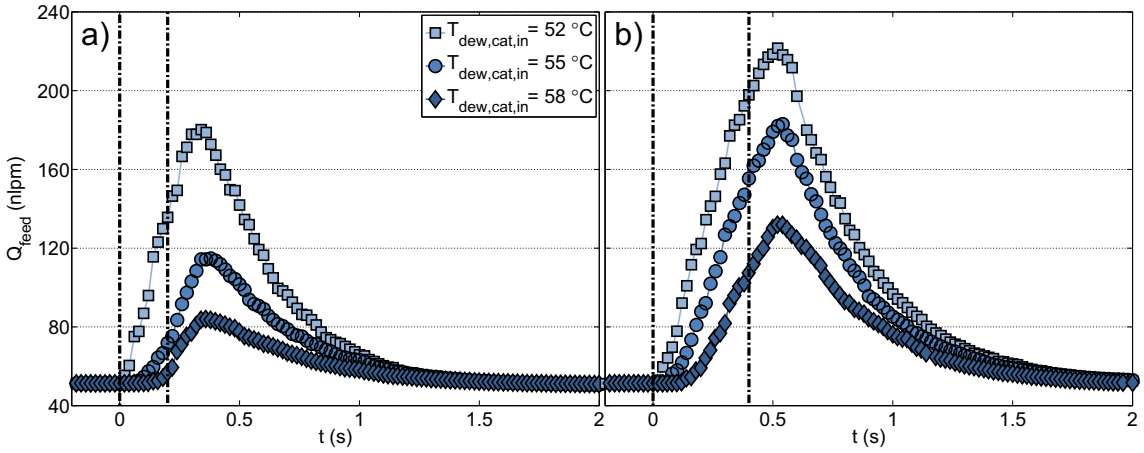

Fig. 4. The hydrogen flow rate profiles averaged from all successfully measured consecutive purge cycles. The cathode inlet dew point temperature was $T_{dew,cat,in} = 52, 55, 58$ °C, the purge time was (a) $t_p = 200$ ms and (b) $t_p = 400$ ms, and the purge triggering criteria was $\Delta E_{trigger} = 3$ mV.

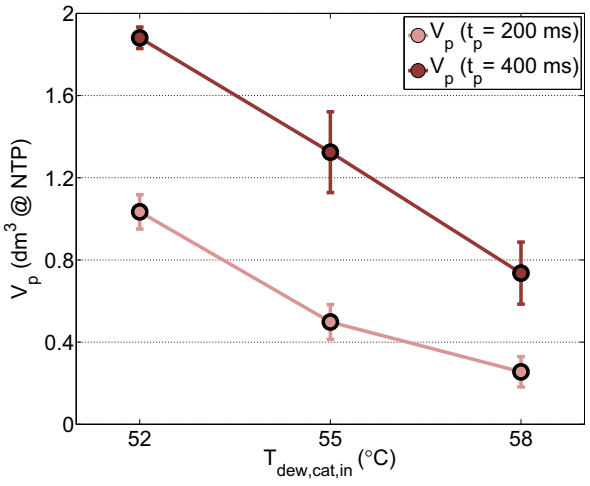

Fig. 5. The volume of anode gas purged (V_p) as a function of humidity level ($T_{dew,cat,in}$). The purge time was t_p = 200, 400 ms and the purge triggering criteria was $\Delta E_{trigger}$ = 3 mV. The error bars show the standard deviation of the measured values.

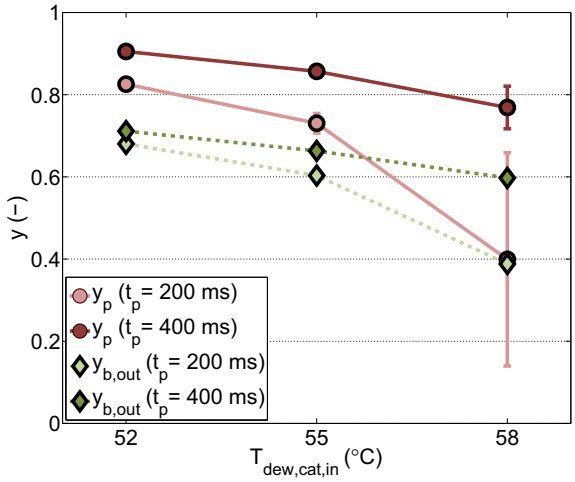

Fig. 6. The hydrogen mole fraction in the purged gas (y_p) and the hydrogen mole fraction at the anode outlet before the purge ($y_{b,out}$) as a function of humidity level ($T_{dew,cat,in}$). The purge time was t_p = 200, 400 ms and the purge triggering criteria was $\Delta E_{trigger}$ = 3 mV. The error bars show the standard deviation of the measured values.

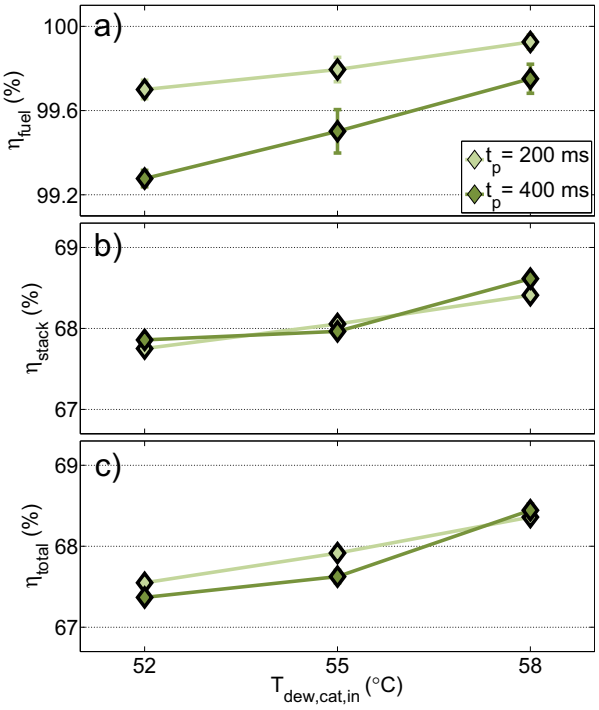

Fig. 8. (a) The fuel efficiency (η_{fuel}, not including fuel cross-over), (b) the stack efficiency (η_{stack}, based on the LHV of hydrogen), and (c) the total efficiency (η_{total}) as a function of humidity level ($T_{dew,cat,in}$). The purge time was t_p = 200, 400 ms and the purge triggering criteria was $\Delta E_{trigger}$ = 3 mV. The error bars show the standard deviation of the measured values.

$$\eta_{total} = \eta_{fuel} \cdot \eta_{stack} \tag{7}$$

As seen in Fig. 8, the stack efficiency accounts for approximately 0.8% of the increase in system efficiency when comparing humid conditions to dry conditions with t_p = 400 ms, while the fuel efficiency accounts for approximately 0.3% although the volume of purged gas changed by a factor of 2.5. The highest system efficiency is achieved when operating the system at the highest humidity level, $T_{dew,cat,in}$ = 58 °C. While it can be concluded that the purged volume might not have a prominent impact on the system total

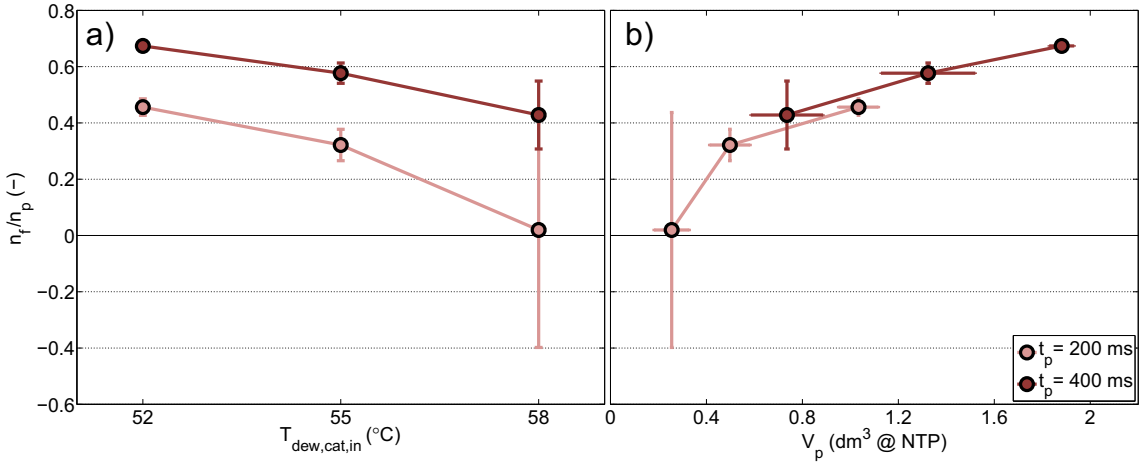

Fig. 7. The fraction of fresh hydrogen in the purged gas (n_f/n_p) (a) as a function of humidity level ($T_{dew,cat,in}$) and (b) as a function of volume purged (V_p). The purge time was t_p = 200, 400 ms and the purge triggering criteria was $\Delta E_{trigger}$ = 3 mV. The error bars show the standard deviation of the measured values.

Table 5
The measured time average reactant dew point temperatures (T_{dew}) and average hydrogen mole fractions in anode loop before and after a purge (y).

↓ $\Delta E_{trigger}$ (mV)	$T_{dew,cat,in}$ (°C)			$T_{dew,cat,out}$ (°C)			$T_{dew,an,in}$ (°C)			$T_{dew,an,out}$ (°C)			y_b (−)			y_a (−)		
$T_{dew,cat,in}$ (°C)/t_p (ms) →	52/200	52/400	55/400	52/200	52/400	55/400	52/200	52/400	55/400	52/200	52/400	55/400	52/200	52/400	55/400	52/200	52/400	55/400
52	52.1	52.0	54.9	64.7	64.4	64.9	47.6	48.1	49.7	60.4	61.4	62.9	0.78	0.80	0.77	0.85	0.88	0.85
55	52.1	52.3	55.0	64.5	65.1	65.9	47.6	48.0	50.2	60.7	60.9	63.7	0.66	0.64	0.62	0.78	0.80	0.76
58	52.0	52.1	54.9	64.8	64.5	65.4	46.1	46.2	49.5	59.5	59.7	63.1	0.56	0.58	0.51	0.70	0.78	0.65

Table 6
The calculated volume of anode gas purged (V_p), anode gas recirculation rate at anode inlet ($Q_{an,in}$), average hydrogen utilization per pass ($\Phi_{H_2,average}$), and fraction of water leaving the stack as liquid water on the anode side (ψ_{H_2O}).

↓ $\Delta E_{trigger}$ (mV)	V_p (dm^3 @ NTP)			$Q_{an,in}$ (NLPM)			$\Phi_{H_2,average}$ (%)			ψ_{H_2O} (%)		
$T_{dew,cat,in}$ (°C)/t_p (ms) →	52/200	52/400	55/400	52/200	52/400	55/400	52/200	52/400	55/400	52/200	52/400	55/400
3	1.03	1.88	1.32	112.5	109.7	110.8	55.8	55.9	56.9	0.1	0.3	3.6
6	0.81	1.33	0.89	109.9	111.2	109.1	62.5	61.4	64.7	0.4	0.5	2.5
9	0.75	1.49	0.58	107.8	107.1	108.0	69.0	65.9	72.9	0.0	0.0	2.9

efficiency, it is important in fuel cell system exhaust gas treatment, as discussed by Dehn et al. [2].

The fraction of liquid water leaving the system through the anode purge valve to the total amount of water leaving the system (water entering + water generation) at high humidity levels is substantial, as seen in Table 4, reaching a value of 7.3% under the most humid conditions. This should be taken into account when estimating the water balance and sizing the cathode humidifier in similar system configurations.

3.2. Effect of purge triggering criteria on system efficiency

One of the goals of this study was to determine the optimum trigger criteria from system efficiency point of view. However, as discussed above, a very high fuel efficiency (>99%) can easily be reached even when purge time and trigger voltage are not optimized.

The effect of purge triggering voltage drop on the efficiency and the purged volume can be studied using data from measurements with cathode inlet dew point temperature $T_{dew,cat,in} = 52$ °C and $T_{dew,cat,in} = 55$ °C. However, with $T_{dew,cat,in} = 55$ °C, data could be recorded only with the longer purge ($t_p = 400$ ms). The measured data is shown in Tables 5 and 6, which are organized in the same way as Tables 3 and 4, respectively.

Comparing the average hydrogen flow rate profiles measured using different purge triggering voltage drops in Fig. 9a and b, it is seen that the flow rate profiles with $\Delta E_{trigger} = 6$ mV and $\Delta E_{trigger} = 9$ mV are similar under dry conditions ($T_{dew,cat,in} = 52$ °C). This is true for measurements with both $t_p = 200$ ms and $t_p = 400$ ms. In contrast, under more humid conditions ($T_{dew,cat,in} = 55$ °C), increasing the $\Delta E_{trigger}$ (Fig. 9c) creates a similar effect on the average flow rate profiles as increasing the humidity level (Fig. 4). Since the interval between purges increases with increasing $\Delta E_{trigger}$, these observations suggest that the water accumulation in the flow channels has had time to reach equilibrium when operating the system at $T_{dew,cat,in} = 52$ °C and $\Delta E_{trigger} = 6$ mV.

The suggested equilibrium condition in water accumulation is also observed when comparing the stack efficiencies, i.e. stack voltages, as a function of $\Delta E_{trigger}$ in Fig. 10b. The stack efficiency seems to be constant in the range $\Delta E_{trigger} = 6$–9 mV in dry conditions.

However, in more humid conditions, the stack efficiency is not constant in this range of $\Delta E_{trigger}$. In fact, the stack efficiency seems

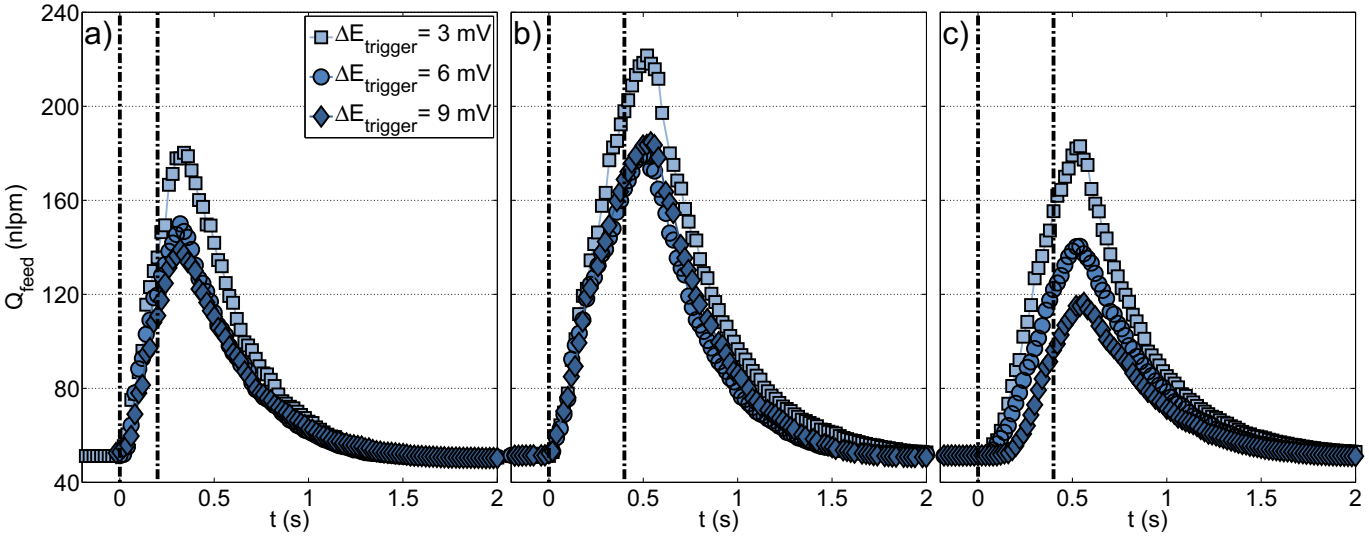

Fig. 9. The hydrogen flow rate profiles averaged from all successfully measured consecutive purge cycles. The cathode inlet dew point temperature and the purge time was (a) $T_{dew,cat,in} = 52$ °C, $t_p = 200$ ms, (b) $T_{dew,cat,in} = 52$ °C, $t_p = 400$ ms, (c) $T_{dew,cat,in} = 55$ °C, $t_p = 400$ ms, and the purge triggering criteria was $\Delta E_{trigger} = 3, 6, 9$ mV.

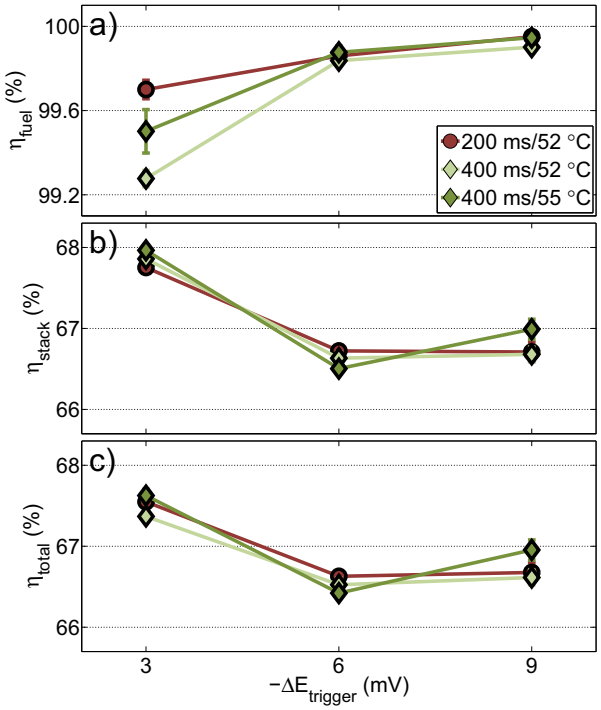

Fig. 10. (a) The fuel efficiency (η_{fuel}, not including fuel cross-over), (b) the stack efficiency (η_{stack}, based on the LHV of hydrogen), and (c) the total efficiency (η_{total}) as a function of purge triggering criteria ($\Delta E_{trigger}$). The purge time was t_p = 200, 400 ms and the humidity level was $T_{dew,cat,in}$ = 52, 55 °C. The error bars show the standard deviation of the measured values.

to increase in the range $\Delta E_{trigger}$ = 6–9 mV. This might be an erroneous result, caused by the stack voltage being very sensitive to the operating conditions, especially to the humidity level inside the stack and to the water accumulation in the flow channels, which were found to reach equilibrium very slowly.

In all measurements, the stack efficiency is found to reach its maximum at $\Delta E_{trigger}$ = 3 mV (Fig. 10b), which is expected because the average voltage drop is the smallest drop used in these experiments. Similarly, in all measurements, the highest fuel efficiency was reached at $\Delta E_{trigger}$ = 9 mV (Fig. 10a), which is due the longest purge interval and the smaller volume purged. The highest total efficiency, however, is reached at $\Delta E_{trigger}$ = 3 mV (Fig. 10c), implying that the stack efficiency through the water balance is the single most important factor in total efficiency, as concluded above.

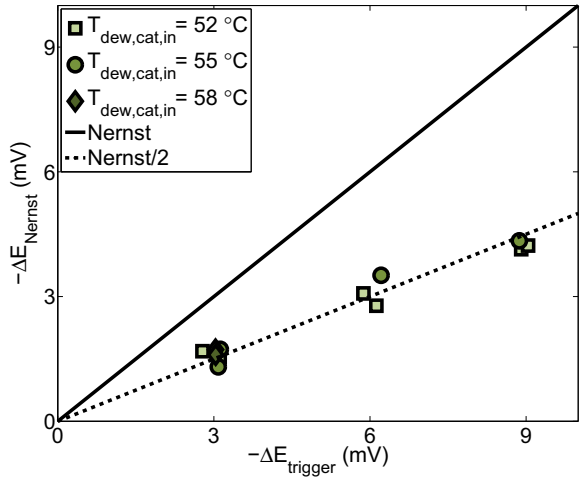

Fig. 11. The measured voltage drop between purges compared to the voltage drop calculated using the measured hydrogen mole fractions and the Nernst equation. The cathode inlet dew point temperature is $T_{dew,cat,in}$ = 52, 55, 58 °C, the purge time is t_p = 200, 400 ms, and the purge triggering criteria is $\Delta E_{trigger}$ = 3, 6, 9 mV.

3.3. Concentration polarization due to N_2 build-up

An important issue in optimizing the design and operation of a PEMFC system is to understand how much voltage loss N_2 build-up is causing on the anode side. In an ideal situation, the dilution is homogeneous throughout the stack. In practice, however, there will be hydrogen concentration gradients between the inlet and outlet as well as between the channel and rib area. In addition, there will be differences between the channels and cells, as flow resistance will be different due to tolerance errors and water accumulation during operation.

Since the hydrogen mole fraction at both the anode inlet and outlet are measured, the theoretical voltage drop due to hydrogen dilution can be calculated using the average hydrogen mole fraction in the Nernst equation. The Nernst equation for a fuel cell using hydrogen as fuel is:

$$E = E^0 - \frac{RT}{2F}\cdot \ln\left(\frac{p_{H_2O}}{p_{H_2}\cdot p_{O_2}^{1/2}}\right) \quad (8)$$

The voltage drop caused by concentration polarization, assuming constant oxygen and water partial pressures, is:

$$\Delta E_{Nernst} = E_2 - E_1 = \frac{RT}{2F}\cdot \ln\left(\frac{p_{H_2,2}}{p_{H_2,1}}\right) \quad (9)$$

As seen in Fig. 11, the voltage drop calculated using the Nernst equation is roughly half of the measured voltage drop and seems to be independent of the humidity level, which indicates that the water accumulation is not highly uneven.

This result suggests that the mass transport resistance for the hydrogen in the gas diffusion layer (GDL) cannot be ignored. Therefore, it can be concluded that mathematical models [21,22], in which the voltage drop is due to simple N_2 build-up and mass transfer resistance is not taken into account, give erroneous estimates of the concentration polarization.

4. Conclusions

In this work, a methodology of reproducibly measuring the purged gas volume and composition was verified and the hydrogen purge was studied as a function of humidity, purge time and purge triggering criteria. The results show that the operating conditions (humidity) are a significant factor for defining the optimum purge strategy. Consequently, in the models for the purge optimization, water accumulation should be taken into account if the stack is operated under such conditions that water accumulation in the flow channels is possible.

It was found that the highest system efficiency is achieved when operating the system under humid conditions and with quite frequent purges, corresponding to low voltage drop allowed between purges.

It could be observed that operating the system in humid conditions, and hence close to conditions where flooding occurs, makes the determination of stack efficiency challenging due to unstable stack performance and long stabilizing times. However, this was also the point of highest system efficiency.

The fuel efficiency, and hence the purge time, in turn, does not affect the system efficiency very much, since the impact of water balance on system efficiency dominates over fuel efficiency. Instead, it is concluded that the purge time should be justified to efficiently

remove the liquid water built-up in the flow channels. Moreover, when operating the system in humid conditions, the amount of water leaving the system as liquid through the anode was found to be significant, thus affecting the humidification of the cathode inlet air.

Furthermore, the theoretical concentration polarization, calculated using the average hydrogen concentration in the flow channels, was found to be roughly half of the measured polarization, indicating a significant mass transport resistance in GDL. However, the mass transport resistance was independent of the humidity level for the stack studied in this work.

The results presented in this paper using the developed methodology are specific to the stack and the system used in this study. In addition, only one current density level and air stoichiometry were studied.

Acknowledgments

This research has been conducted under the “Fuel Cell 2007-2013” technology program of Tekes, the Finnish Funding Agency for Technology and Innovation. The authors would also like to acknowledge their TopDrive project partners.

References

[1] R.K. Ahluwalia, X. Wang, J. Power Sources 171 (2007) 63–71.
[2] S. Dehn, M. Woehr, A. Heinzel, in: 2011 IEEE Vehicle Power and Propulsion Conference, VPPC 2011 (2011).
[3] K.D. Baik, M.S. Kim, Int. J. Hydrogen Energy 36 (2011) 732–739.
[4] A. Mokmeli, S. Asghari, Int. J. Hydrogen Energy 35 (2010) 9276–9282.
[5] J.B. Siegel, A.G. Stefanopoulou, in: American Control Conference (ACC), 2010 (2010), pp. 6606–6611.
[6] R. Anderson, L. Zhang, Y. Ding, M. Blanco, X. Bi, D.P. Wilkinson, J. Power Sources 195 (2010) 4531–4553.
[7] F.N. Büchi, Heterogeneous cell ageing in polymer electrolyte fuel cell stacks, in: F.N. Büchi, M. Inaba, T.J. Schmidt (Eds.), Polymer Electrolyte Fuel Cell Durability, Springer, New York, 2009, pp. 431–439.
[8] K. Promislow, J. St-Pierre, B. Wetton, J. Power Sources 196 (2011) 10050–10056.
[9] J.B. Siegel, D.A. McKay, A.G. Stefanopoulou, in: Proceedings of the 6th International Conference on Fuel Cell Science, Engineering, and Technology, 2008, pp. 757–768.
[10] J.B. Siegel, S.V. Bohac, A.G. Stefanopoulou, S. Yesilyurt, J. Electrochem. Soc. 157 (2010) B1081–B1093.
[11] J.W. Choi, Y. Hwang, S.W. Cha, M.S. Kim, Int. J. Hydrogen Energy 35 (2010) 12469–12479.
[12] A. Manokaran, S. Pushpavanam, P. Sridhar, S. Pitchumani, J. Power Sources 196 (2011) 9931–9938.
[13] H. Karimäki, L.C. Pérez, K. Nikiforow, T.M. Keränen, J. Viitakangas, J. Ihonen, Int. J. Hydrogen Energy 36 (2011) 10179–10187.
[14] L. Dumercy, M.C. Péra, R. Glises, D. Hissel, S. Hamandi, F. Badin, J.M. Kauffmann, Fuel Cells 4 (2004) 352–357.
[15] K.M. Adegnon, Y. Dube, K. Agbossou, Canadian Conference on Electrical and Computer Engineering (2009) 716–719.
[16] D.A. McKay, J.B. Siegel, W. Ott, A.G. Stefanopoulou, J. Power Sources 178 (2008) 207–222.
[17] M. Minutillo, A. Perna, Int. J. Energy Res. 32 (2008) 1297–1308.
[18] E.A. Müller, F. Kolb, L. Guzzella, A.G. Stefanopoulou, D.A. McKay, J. Fuel Cell Sci. Technol. 7 (2010) 0210131–02101311.
[19] T. Pokphet, W. Khan-ngern, J. Charoensuk, International Conference on Electrical Engineering/Electronics Computer Telecommunications and Information Technology (2010) 88–92.
[20] K. Nikiforow, M.Sc. Thesis. Helsinki University of Technology (2010), URL: http://lib.tkk.fi/Dipl/2010/urn100359.pdf, [last accessed 05.07.2012].
[21] J.P. Torreglosa, F. Jurado, P. García, L.M. Fernández, Int. J. Hydrogen Energy 36 (2011) 7628–7640.
[22] R. Seyezhai, B.L. Mathur, Int. J. Hydrogen Energy 36 (2011) 15029–15043.